Available online at www.sciencedirect.com

SciVerse ScienceDirect

Journal of the European Ceramic Society 32 (2012) 1291–1298

www.elsevier.com/locate/jeurceramsoc

Preparation, cross-linking and ceramization of AHPCS/Cp_2ZrCl_2 hybrid precursors for SiC/ZrC/C composites

Zhaoju Yu[a,*], Le Yang[a,b], Junying Zhan[a], Cong Zhou[a], Hao Min[a], Qiang Zheng[a], Haiping Xia[a,b]

[a] *College of Materials, Key Laboratory of High Performance Ceramic Fibers (Xiamen University), Ministry of Education, Xiamen 361005, China*
[b] *College of Chemistry & Chemical Engineering, Xiamen University, Xiamen 361005, China*

Received 27 July 2011; received in revised form 8 December 2011; accepted 11 December 2011
Available online 13 January 2012

Abstract

SiC/ZrC/C composites were prepared via pyrolysis of a polymeric precursor, namely AHPCS/Cp_2ZrCl_2 hybrid precursor prepared by the blend of allylhydridopolycarbosilane (AHPCS) and bis(cyclopentadienyl) zirconium dichloride (Cp_2ZrCl_2). The cross-linking and polymer-to-ceramic conversion of as-synthesized AHPCS/Cp_2ZrCl_2 were characterized by means of FTIR, ^{13}C NMR, TGA, EDS, Raman spectroscopy and XRD. It is suggested that dehydrocoupling, hydrosilylation and dehydrochlorication are involved in the cross-linking of the hybrid precursor, which is responsible for a relatively high ceramic yield of 75.5% at 1200 °C. The polymer-to-ceramic conversion is complete at 900 °C, and it gives an amorphous ceramic. Further heating at 1350 °C induces partial crystallization, and then the characteristic peaks of β-SiC and cubic ZrC appear at 1600 °C. The effect of the composition of the hybrid precursor is also studied in the work.

Keywords: AHPCS/Cp_2ZrCl_2 hybrid precursors; Precursors-organic; Thermal properties; Carbides; Composites

1. Introduction

Silicon carbide (SiC) ceramic has been widely applied in high technology fields such as advanced aviation aircraft structure parts, high-temperature engines, turbines, atomic reactor walls, because of its superior physical and mechanical performance such as high intensity, high modulus, high temperature resistant.[1] However, with the development of science and technology, higher requests to the properties of SiC ceramics put forward, and the main method for preparation of high-performance SiC ceramics is the introduction of heterogeneous element to SiC ceramics, which can enhance the comprehensive performance of the SiC ceramics.[2] Zirconium carbide (ZrC) which is similar to SiC is also known as high refractory ceramics with good thermomechanical properties.[3,4] Thus it can be seen if zirconium is introduced to SiC ceramics which can form SiC and ZrC composites, the combination of the passivating character of SiC and the high melting temperature, hardness and thermal stability of ZrC should generate a kind of high-performance ceramics.[5]

To date, different approaches have been designed to obtain the SiC/ZrC composites, the key point of the approach is the synthesis of precursors containing zirconium. The pyrolysis of an organosilicon polymer in the presence of a metal oxide has been used as a way to obtain Si/C/M (M = Ti, Zr, Al, etc.) multipart ceramics.[6–8] On the other hand, it has also been reported that reaction of polycarbosilane with zirconium (IV) acetylacetonate yields a polyzirconocarbosilane which can be used as the precursor of Si–Zr–C–O ceramic fibers of high tensile strength at high temperatures.[9] However, all of the polymeric precursors mentioned above contain oxygen which would influence the mechanical properties at high temperatures. Recently, Tsirlin et al.[10] chose $ZrCl_4$, Cp_2ZrCl_2, $Zr[N(C_2H_5)_2]_4$, $Zr(CH_2C_6H_5)_4$ and $\{[Si(CH_3)_2]_x–[–Si(CH_3)H–CH_2–]_y\}_n$ (x, $y = 1–8$, $n = 2–6$, $M = 300–600$) as raw materials to obtain non-oxide precursors successfully. Amoros et al.[11] proposed in their work to study the role of bis(cyclopentadienyl)-metal complexes as an alternative source of metal to obtain Si/C/M ceramics. They reported their first results about the reactivity of bis(cyclopentadienyl)-metal dichloride (Cp_2MCl_2, M = Ti, Zr, Hf) versus poly(dimethylsilane) PDMS and

---

[*] Corresponding author.
E-mail address: zhaojuyu@xmu.edu.cn (Z. Yu).

doi:10.1016/j.jeurceramsoc.2011.12.015

poly(dimethylcarbosilane) (PCS) and their application to synthesis of new ceramics based on Si/C/M (M = Ti, Zr, Hf). It revealed that the metal complex can be incorporated into the PDMS and PCS polymer chains by HCl elimination. However, the ceramic yield of a mixture of Cp_2MCl_2 (M = Ti, Zr, Hf) and PCS is only about 30% at 900 °C.

As is well known, liquid hyperbranched PCSs can be regarded as excellent effective precursors especially for a matrix source because of their unique structures and favorable properties, such as lower viscosities, more favorable solubilities, and larger amounts of reactive end-functional groups.[12] In our previous work, we successfully synthesized a series of HBPCSs such as allylhydridopolycarbosilane (AHPCS), ethynylhydridopolycarbosilane (EHPCS) and propargylhydrido-polycarbosilane (PHPCS) by the one-pot synthesis with chlorosilanes and allyl chloride, ethynylmagnesium bromide or propargyl chloride as the starting materials, and the composition of the HBPCSs can be tailored by controlling the amount of the comomers.[13–16] The polymer-to-ceramic conversion of the HBPCS for SiC ceramics was further studied.[17–19]

Based on the findings that both Si–Si dehydrocoupling (the 1,1-elimination of molecular hydrogen from SiH_n groups) and hydrosilylation (a reaction between Si–H and vinyl groups) were effectively improved with bis(cyclopentadienyl)-metal complexes as catalysts,[20–23] we prepared a hybrid precursor of AHPCS/Cp_2ZrCl_2 for the first time. On one hand, Cp_2ZrCl_2 was used as a new source of Zr to Si/C/Zr ceramic composites. On the other hand, the cross-linking of AHPCS which contains a large amount of C=C groups and $Si–H_x$ groups could be improved with Cp_2ZrCl_2 as a catalyst, involving Si–Si dehydrocoupling and hydrosilylation reactions. Herein, we report our first results about the reactivity of Cp_2ZrCl_2 versus AHPCS and their application to the synthesis of new ceramic composites on SiC/ZrC/C composites.

2. Experimental

2.1. Materials

All manipulations were carried out using standard high-vacuum or insert-atmosphere techniques as described by Shriver and Drezdzon.[24] AHPCS with a composition formula $[SiH_{1.26}(CH_3)_{0.60}(CH_2CH{=}CH_2)_{0.14}CH_2]_n$ was prepared, as previously described, by a one-pot synthesis with $Cl_2Si(CH_3)CH_2Cl$, Cl_3SiCH_2Cl, and $CH_2{=}CHCH_2Cl$ as the starting materials.[13,14] AHPCS used in this work had a number-average molecular weight of ca. 700 and a polydispersity index of 1.96. Cp_2ZrCl_2 was purchased from J&K and stored in fridge under 4 °C until use. Chloroform ($CHCl_3$) was distilled prior to use. Other commercially available reagents were used as received.

2.2. Preparation and cross-linking of AHPCS/Cp_2ZrCl_2 hybrid precursors

Preparation and cross-linking of AHPCS/Cp_2ZrCl_2 hybrid precursors were carried out in a Schlenk flask with a magnetic stirrer and an argon inlet. One typical synthesis of the hybrid precursor was described as the following procedure. 0.6 g Cp_2ZrCl_2 was introduced into a 150 mL Schlenk flask in an argon atmosphere, and then 30 mL $CHCl_3$ was added to solve Cp_2ZrCl_2 until a clear colorless solution was obtained. Subsequently, 2.4 g AHPCS was introduced into the Schlenk flask with stirring at room temperature, and then a pale yellow solution was obtained. The weight ratio of Cp_2ZrCl_2 to AHPCS was 1/4, 1/3 and 1/2, and the samples are abbreviated as AZ-1, AZ-2 and AZ-3, correspondingly. After the $CHCl_3$ solvent was stripped off under vacuum at 60 °C to form a yellow AHPCS/Cp_2ZrCl_2 slurry in the Schlenk flask. Finally, the Schlenk flask was heated in a 170 °C oil bath. The resultant AHPCS/Cp_2ZrCl_2 slurry solidified immediately into a compact, light brown, rubbery solid and was kept at this temperature for 6 h. These cross-linked samples of AZ-1, AZ-2 and AZ-3 were used both for TGA and for a macroscopic pyrolysis.

2.3. Pyrolysis of AHPCS/Cp_2ZrCl_2 hybrid precursors

With the pyrolysis temperature (T_p) of 900 °C, the cross-linked sample was put in an alumina boat and heated in a glass silica tube under an argon flow. The temperature was progressively raised up to T_p at a rate of 5 °C/min and kept at this value for 2 h. For $T_p > 900$ °C, the sample (pre-pyrolyzed at 900 °C) was put in a graphite crucible and heated in a tube furnace in argon. The pre-pyrolyzed sample was heated rapidly to T_p at a rate of 40 °C/min and kept at this temperature for 2 h. After pyrolysis, the resulting ceramic was furnace-cooled to RT.

2.4. Characterization

Fourier transform infrared spectroscopy (FTIR) spectra were recorded on Nicolet Avator 360 apparatus (Nicolet, Madison, WI) with KBr plates for liquid samples and KBr discs for solid samples. Nuclear magnetic resonance (NMR) experiments were carried out on a Bruker AV 300 MHz spectrometer (Bruker, Germany) operating at 75.46 MHz for carbon-13 (^{1}H-decoupling). The specimen used for ^{13}C NMR was dissolved in $CDCl_3$ solution. The ^{13}C chemical shifts were referred to tetramethylsilane (TMS) (assigned to 0 ppm). The solid-state ^{13}C-magic angle spinning (MAS) NMR experiments were also performed on a Bruker AV 300 NMR spectrometer using a 4.0 mm Bruker double resonance MAS probe. The samples were spun at 5.0 kHz. The ^{13}C isotropic chemical shifts were referenced to the carbonyl carbon of glycine (assigned to 173.2 ppm). Thermal analysis of the samples was performed on a thermal gravimetric analysis (TGA) (Netzsch STA 409EP, Netzsch, Germany) in argon gas with a heating rate of 10 °C/min ranging from room temperature (RT) to 1200 °C. X-ray diffraction (XRD) studies were executed on a PANalytical X'Pert PRO diffractometer (PANalytical, Netherlands) with Cu Kα radiation. The specimens were continuously scanned from 10° to 90° (2θ) at a speed of $0.0167°\ s^{-1}$. The apparent mean grain size of the β-SiC and cubic ZrC crystalline phase was calculated from the width of the (1 1 1) diffraction peak at mid-height, according to the Scherer equation.[25] The elemental analysis of

Table 1
Si—H reaction degree of a series of AZ hybrid precursors.

Polymeric precusors	Cp_2ZrCl_2 content[a]	Zirconium content (%)[b]	A(Si—H)/A(Si—CH_3)	P_{Si-H} (%)[c]
Original AHPCS	0	0	19.10	0
Cross-linked AHPCS[d]	0	0	18.99	0.58
Cross-linked AZ-1[d]	1/4	6.24	14.96	21.68
Cross-linked AZ-2[d]	1/3	7.80	13.31	30.31
Cross-linked AZ-3[d]	1/2	10.40	9.79	48.74

[a] Weight ratio of Cp_2ZrCl_2 to AHPCS in feed.
[b] Weight percent of zirconium to precursor in feed.
[c] Reaction degree of Si—H groups measured by FT IR.
[d] Treated at 170 °C for 6 h.

ceramics was performed by an energy dispersive spectrometer (EDS, JEOL, Japan). Moreover, the ceramic composition was determined by bulk chemical analysis as well as EDS. Elemental analyses were carried out by a Horiba Carbon/Sulfur Analyzer EMIA-320V (Horiba, Japan) for carbon element, a Horiba Oxygen/Nitrogen Analyzer EMGA-620W for oxygen element, and Elemental Analyzer EA/MA1110 (Carlo Erba, Milan, Italy) for hydrogen and chloride elements. The zirconium content of the ceramic was determined by ethylenediaminetetraacetic acid (EDTA) complexometric titration after melting the samples with potassium hydroxide (KOH). The silicon content was calculated as the difference of the sum of the measured carbon, oxygen, and zirconium content to 100%. Raman spectra were recorded on a Raman spectrometer (TriVista CRS557, Princeton, USA).

3. Results and discussion

3.1. Cross-linking of hybrid precursors

The cross-linking reaction of AHPCS/Cp_2ZrCl_2 hybrid precursors was investigated by FTIR (Fig. 1). The hybrid precursors exhibited typical AHPCS characteristics and the peaks observed in these spectra are assigned according to the literatures,[14,17,18] as follows: 3077 cm^{-1} (w, C–H stretch in –CH=CH_2), 1630 cm^{-1} (w, C=C stretch in –CH=CH_2), 2140 cm^{-1} (vs, Si–H stretch), 940 cm^{-1} (vs, Si–H bending), 2950, 2873 cm^{-1} (s, CH_3 stretch), 2920 cm^{-1} (s, CH_2 stretch), 1400, 1250 cm^{-1} (Si–CH_3 deformation), 1355 cm^{-1} (s, Si–CH_2–Si deformation), 1040 cm^{-1} (vs, Si–CH_2–Si stretch), 800 cm^{-1} (vs, Si–C stretch). From a comparison of the FTIR spectra of cross-linked AHPCS/Cp_2ZrCl_2 hybrid precursors shown in Fig. 1(c)–(e) with those of AHPCS (Fig. 1(a)) and Cp_2ZrCl_2 (Fig. 1(f)), it is observed cross-linked hybrid precursors contain characteristic peaks of AHPCS and Cp_2ZrCl_2. Several appearances of absorption peak at 1438 cm^{-1} (C–C stretch in Cp rings), 1016 cm^{-1} (C–H in plane deformation in Cp rings), 814 cm^{-1} (C–H out of plane deformation in Cp rings) are observed.[26] It indicates that Cp_2ZrCl_2 is successfully introduced into AHPCS because the trend of Cp_2ZrCl_2 to sublimate is significant above 160 °C.[27]

It is worth mentioning that Si–H stretch (2140 cm^{-1}) peak significantly decreases after the introduction of Cp_2ZrCl_2. To investigate the reaction degree of Si–H bonds (P_{Si-H}) of the

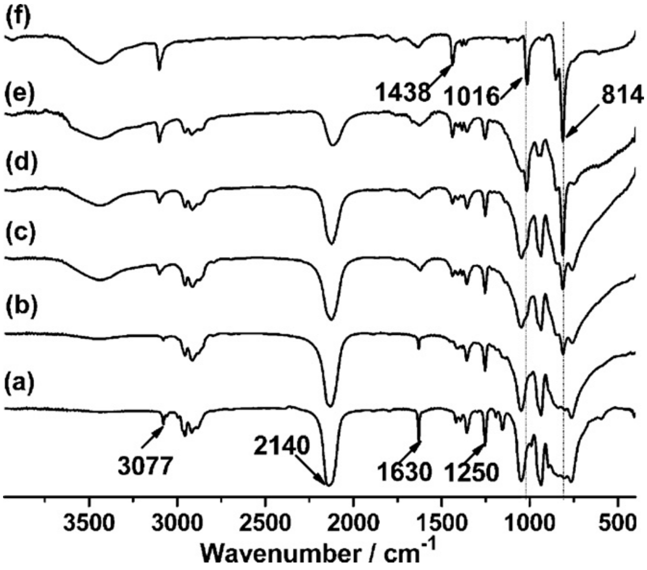

Fig. 1. FTIR spectra of (a) original AHPCS, (b) cross-linked AHPCS, (c) cross-linked AZ-1, (d) cross-linked AZ-2, (e) cross-linked AZ-3, and (f) Cp_2ZrCl_2.

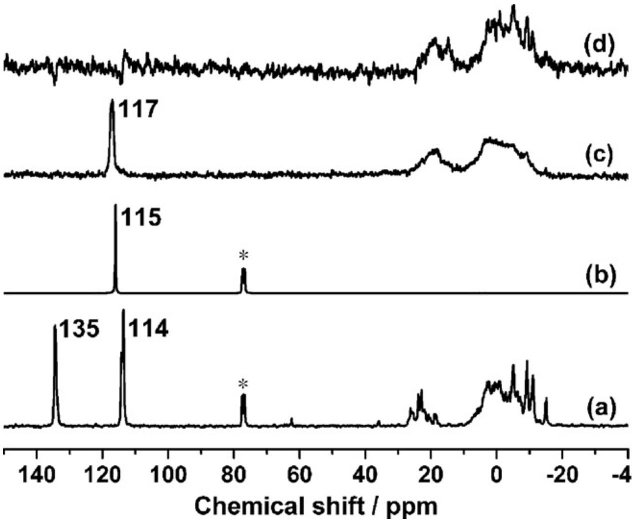

Fig. 2. ^{13}C NMR spectra of (a) the soluble AHPCS (*$CDCl_3$ solvent), (b) Cp_2ZrCl_2 (*$CDCl_3$ solvent) and solid-state ^{13}C MAS NMR spectra of (c) cross-linked AZ-2, and (d) cross-linked AHPCS.

hybrid precursors and the original AHPCS, $P_{Si\text{–}H}$ was measured and the results are shown in Table 1.

Herein, the intensity ratio of the peaks at 2140 cm^{-1} (Si–H) to that at 1250 cm^{-1} ($Si\text{–}CH_3$) are denoted as *A(Si–H)/A(Si–CH₃)*. The $Si\text{–}CH_3$ bond should not be involved in the chemical reaction at 170 °C, therefore, the value of $A(Si\text{–}H)/A(Si\text{–}CH_3)$ indicates the Si–H content. The $P_{Si\text{–}H}$ was determined according to our previous work.[15] It shows that the $A(Si\text{–}H)/A(Si\text{–}CH_3)$ and the $P_{Si\text{–}H}$ gradually decrease with the increase of zirconium contents in feed, indicating that Si–H bonds are involved in the cross-linking. The consumption of Si–H is due to the Si–Si dehydrocoupling (Eq. (1)) and hydrosilylation (Eq. (2)), which is obviously improved by the introduction of Cp_2ZrCl_2 into the hybrid precursors. On the other hand, Cp_2ZrCl_2 can be incorporated into the PCS polymer chains by HCl elimination namely dehydrochlorication (Eq. (3)),[11] which also contributes to the consumption of Si–H.

onset of thermal decomposition for AZ hybrid precursor is about 150 °C, which is consistent with the sublimation point of Cp_2ZrCl_2. At 350 °C, a weight loss of AHPCS is 8.4%, whereas those of AZ-1, AZ-2, and AZ-3 are 11.3%, 15.9%, and 23.3%, respectively. The weight loss of AZ hybrid precursors is higher than that of AHPCS, and it increases with the Cp_2ZrCl_2 contents in feed increasing, which might be due to that the trend of Cp_2ZrCl_2 to sublimate increases. Over the 350–500 °C region, the weight loss of AHPCS, AZ-1, AZ-2, and AZ-3 are 20.8%, 3.0%, 3.0%, and 3.2%, correspondingly. Over the 500–900 °C region, weight loss of AHPCS (9.0%) closely matches those of AZ hybrid precursors (8.0–9.0%). Over the 900–1200 °C region, no obvious weight loss is observed for both AHPCS and AZ, indicating the completion of polymer-to-ceramic conversion. It is worth mentioning that over the 350–500 °C, significant differences in weight loss are observed for the AHPCS and AZ hybrid precursors, which is responsible for the difference in final ceramic yields. According to the literature,[28] it is found that over the 300–500 °C range, the evolution of volatile gases CH_3CH_3, SiH_4 and CH_3SiH_3 is responsible for the weight loss of the AHPCS. It seems that the evolution of these three types gases is suppressed in the AZ hybrid precursors. As a result, the

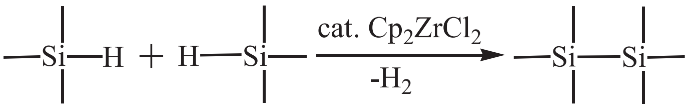

$$-\mathrm{Si}-\mathrm{H} + \mathrm{H}-\mathrm{Si}- \xrightarrow[-\mathrm{H_2}]{\text{cat. } \mathrm{Cp_2ZrCl_2}} -\mathrm{Si}-\mathrm{Si}- \tag{1}$$

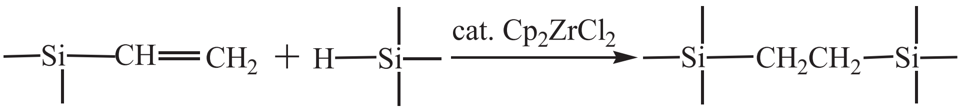

$$-\mathrm{Si}-\mathrm{CH}{=}\mathrm{CH_2} + \mathrm{H}-\mathrm{Si}- \xrightarrow{\text{cat. } \mathrm{Cp_2ZrCl_2}} -\mathrm{Si}-\mathrm{CH_2CH_2}-\mathrm{Si}- \tag{2}$$

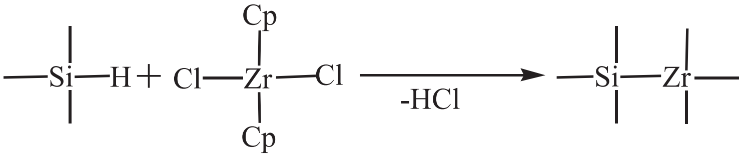

$$-\mathrm{Si}-\mathrm{H} + \mathrm{Cl}-\underset{\mathrm{Cp}}{\overset{\mathrm{Cp}}{\mathrm{Zr}}}-\mathrm{Cl} \xrightarrow[-\mathrm{HCl}]{} -\mathrm{Si}-\mathrm{Zr}- \tag{3}$$

In addition, ^{13}C NMR spectra of original AHPCS, Cp_2ZrCl_2 and solid-state ^{13}C MAS NMR spectra of cross-linked hybrid precursor AZ-2 and AHPCS treated at 170 °C are shown in Fig. 2.

The ^{13}C NMR assignment of AHPCS was described elsewhere.[13,14] In comparison with the ^{13}C MAS NMR spectrum of the cross-linked AHPCS, the AZ-2 shows one additional resonance at 117 ppm, which is a little different from the cyclopentadienyl signal at 115 ppm of Cp_2ZrCl_2. It is believed that the chemical shift from 115 ppm to 117 ppm could further confirm the introduction of Cp_2ZrCl_2 into AHPCS chains.

In summary, it is suggested that Cp_2ZrCl_2 was successfully introduced into AHPCS chains in combination of FT IR and NMR results, which is consistent with the previous finding based on the incorporation of the bis(cyclopentadienyl)-metal dichloride (M = Ti, Zr, Hf) into PCS by dehydrochlorication reaction.

3.2. *Ceramization of hybrid precursors*

In order to understand the thermal behavior during the ceramization of the cross-linked hybrid precursor, TGA was measured and the result is shown in Fig. 3.

The 1200 °C ceramic yield of AZ-1, AZ-2, AZ-3 and AHPCS reached 75.5%, 71.4%, 64.5% and 60.5%, respectively, indicating that the ceramic yield increases significantly by the introduction of Cp_2ZrCl_2. Careful examination shows that the

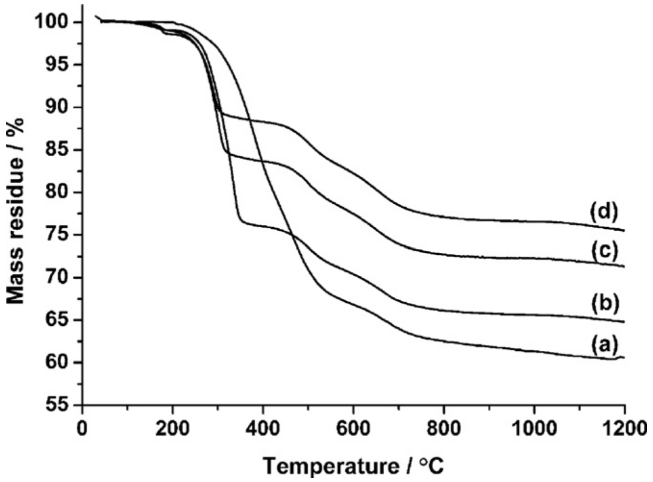

Fig. 3. TGA curves of (a) cross-linked AHPCS, (b) cross-linked AZ-3, (c) cross-linked AZ-2, and (d) cross-linked AZ-1.

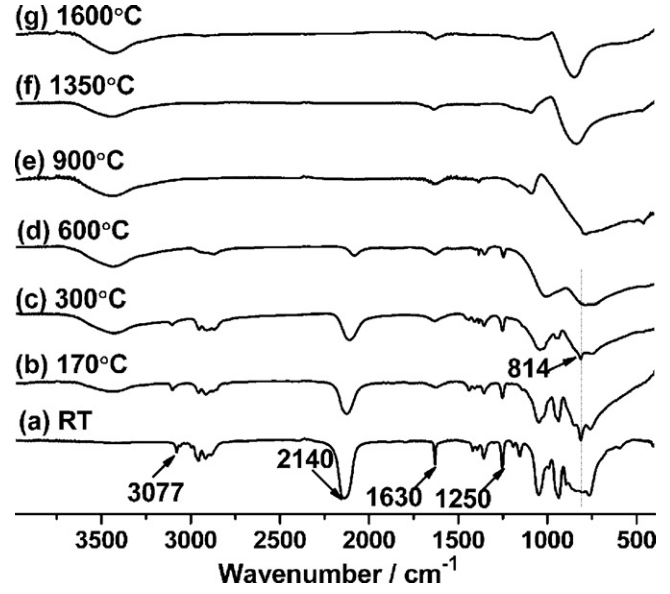

Fig. 4. FTIR spectra of (a) AHPCS at room temperature and AZ-2 treated at (b) 170 °C, (c) 300 °C, (d) 600 °C, (e) 900 °C, (f) 1350 °C, and (g) 1600 °C.

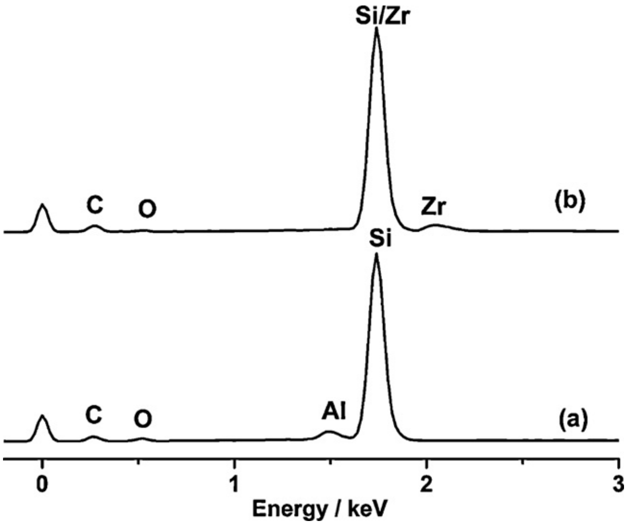

Fig. 5. EDS elemental analysis of 1600 °C ceramics derived from (a) original AHPCS and (b) AZ-3 hybrid precursor.

introduction of Cp_2ZrCl_2 to the hybrid precursor improves the final ceramic yield.

In order to understand the structural evolution of AZ hybrid precursors during the polymer-to-ceramic conversion, FTIR were thus measured (Fig. 4). It is readily observed that the absorption of Si–H at 2140 cm^{-1} and C=C at 1630 cm^{-1} in AZ-2 hybrid precursor markedly decreases after heat treatment at 170 °C in comparison with that at room temperature. At 300 °C, the absorption of Si–H and C=C decreases further. In the FTIR spectrum at 600 °C, the absorption of $Si–CH_3$ at 1250 cm^{-1} and C–H in Cp rings at 814 cm^{-1} gradually reduces, which should be attributed to the decomposition of organic side groups, meanwhile, the intensity of Si–H at 2140 cm^{-1} decreases markedly and the Si–H bending at 940 cm^{-1} almost vanishes. At 900 °C, only one broad peak at around 800 cm^{-1} (attributed to SiC_4) is retained, and other bands such as 1250 cm^{-1} (assigned to $Si–CH_3$) and even 1040 cm^{-1} (from $Si–CH_2–Si$ functionalities), are no longer observed in the FTIR spectrum. It is believed that the conversion from polymer-to-ceramic is complete at around 900 °C, which well matches the TGA result. Further heating to 1350 and 1600 °C led to the sharpening of the SiC band and a shift in its position from 780 to 850 cm^{-1}, consistent with the formation of crystalline SiC. In summary, the AZ hybrid precursor underwent the cross-linking, organic to inorganic transition and conversion of amorphous to crystalline phase during the heat treatment.

To analyze the ceramic composition, the EDS elemental analysis of the 1600 °C ceramics was measured and the result is shown in Fig. 5. The EDS spectrum of the AZ-derived ceramic exhibits characteristic peaks of silicon, zirconium, oxygen and carbon, confirming that the ceramic only contain silicon, zirconium, carbon and oxygen elements.

The Zr contents of Si/C/Zr ceramics, as locally assessed by EDS, are presented in Fig. 6. It is worth mentioning that the ceramic yield increases linearly with the Zr content of precursor increasing. Therefore, the Zr content in ceramics could be readily controlled by varying the Zr content in feed.

In more detail, the chemical compositions of AZ-derived ceramics at 1600 °C were also determined by bulk chemical analysis, and the results are shown in Table 2. The 1600 °C ceramics derived from AHPCS, AZ-1, AZ-2 and AZ-3 are presented as AH-1600 °C, AZ-1-1600 °C, AZ-2-1600 °C and AZ-3-1600 °C, respectively. The AZ-derived ceramics are totally chlorine and hydrogen-free. It is worth mentioning that the Zr contents are well consistent with the EDS results. Moreover, the carbon contents in the ceramics increase with the weight ratio of AHPCS/Cp_2ZrCl_2 increasing because of the higher amount of Cp_2ZrCl_2 introduced into the hybrid precursor.

3.3. Crystallization behavior of AZ-derived ceramics

In order to investigate the crystallization of AZ-derived ceramics, XRD patterns of the samples were measured. Fig. 7

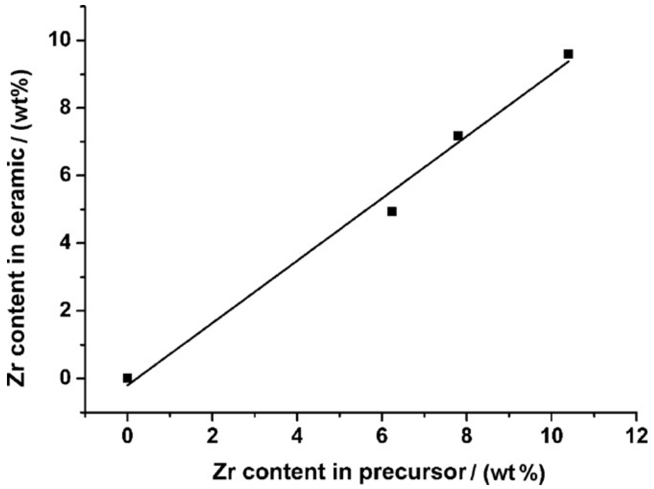

Fig. 6. Dependence of Zr content in 1600 °C ceramics on Zr content in hybrid precursor.

Table 2
Chemical composition of 1600 °C ceramics from bulk chemical analysis.

No.	Si content[a]		C content[b]		O content[c]		Zr content[d]		Average formula
	wt%	at%	wt%	at%	wt%	at%	wt%	at%	
AH-1600 °C	61.25	40.63	37.15	57.51	1.60	1.86	0	0	$SiC_{1.42}O_{0.046}$
AZ-1-1600 °C	54.81	36.72	38.53	60.24	1.72	2.02	4.94	1.02	$SiC_{1.64}Zr_{0.028}O_{0.055}$
AZ-2-1600 °C	51.97	35.02	39.07	61.44	1.73	2.04	7.23	1.50	$SiC_{1.75}Zr_{0.043}O_{0.058}$
AZ-3-1600 °C	45.27	29.59	44.12	67.29	1.05	1.20	9.56	1.92	$SiC_{2.27}Zr_{0.065}O_{0.040}$

[a] Determined by the difference.
[b] Measured by Carbon/Sulfur Analyzer.
[c] Measured by Oxygen/Nitrogen Analyzer.
[d] Measured by EDTA complexometric titration after melting the sample with KOH.

shows that the ceramic at 900 °C is amorphous and highly disordered. Further heating at 1200 °C causes a broad peak at 36°, indicating the incomplete crystallization and the formation of a local order SiC_4. At 1350 °C, the intensity of broad peak at 36° increases, which indicates that the resultant SiC_4 is more ordered in comparison with that at 1200 °C, in the meantime, weak peaks appear at 33.2° (1 1 1), 38.5° (2 0 0), 55.7° (2 2 0), 66.4° (3 1 1) and 69.7° (2 2 2) and it means that cubic ZrC generates in the ceramic.[11] Further heating to 1600 °C led to the sharpening of characteristic peaks of β-SiC and cubic ZrC. According to the Scherer equation, the β-SiC grain size of AZ-2-derived ceramics is 16.5 nm, whereas the cubic ZrC grain size is 53.9 nm. Moreover, graphite signals at 27° are visible at all temperatures from 900 to 1600 °C. As can be expected, SiC/ZrC/C composites were successfully prepared via the pyrolysis of AHPCS/Cp_2ZrCl_2 hybrid precursor.

Raman spectroscopy is one of the most sensitive spectral methods for the characterization of the different modifications of carbon. Fig. 8 shows the Raman spectra of AZ-2-derived ceramics to get insight into the evolution of free carbon with different pyrolysis temperatures. At 900 °C, signals of free

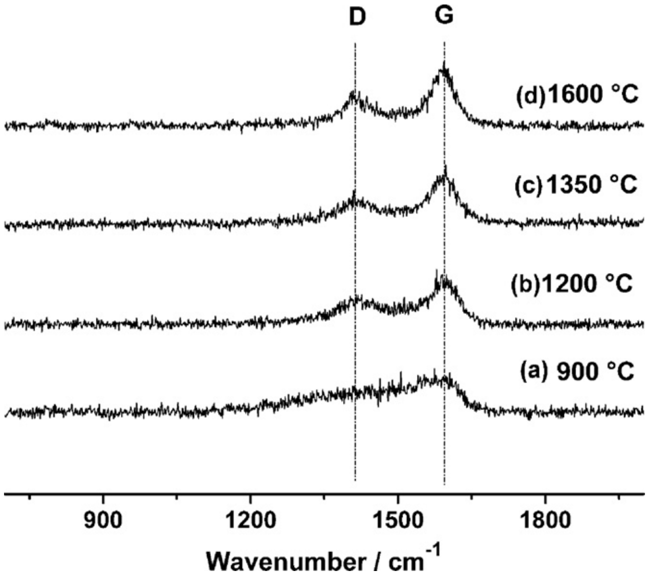

Fig. 8. Raman spectra of (a) 900 °C, (b) 1200 °C, (c) 1350 °C, and (d) 1600 °C ceramics derived from cross-linked AZ-2.

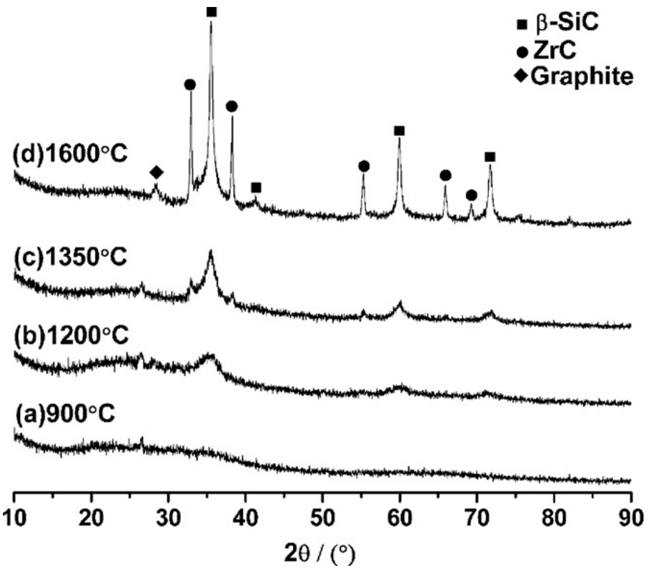

Fig. 7. XRD patterns of (a) 900 °C, (b) 1200 °C, (c) 1350 °C, and (d) 1600 °C ceramics derived from cross-linked AZ-2.

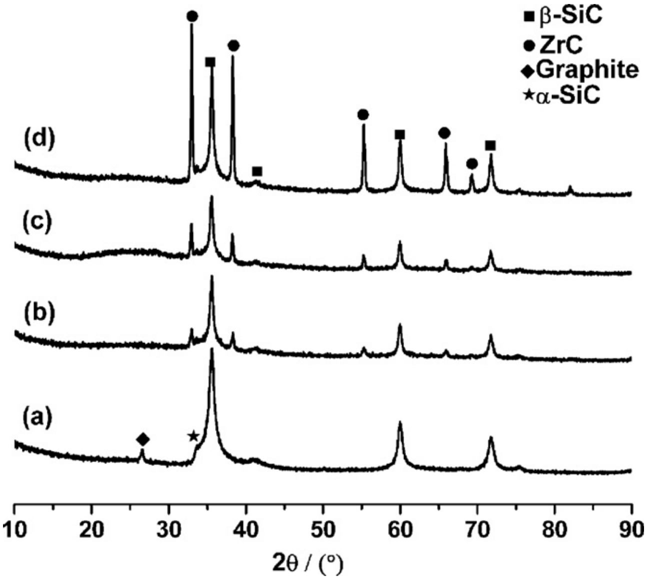

Fig. 9. XRD patterns of 1600 °C ceramics derived from cross-linked (a) AHPCS, (b) AZ-1, (c) AZ-2, and (d) AZ-3.

carbon are observed. Further heating to 1200 °C, two peaks centered around 1350 cm^{-1} and 1600 cm^{-1} are discernable, which correspond to the D and G peaks observed in free carbon.[29,30] The peak at 1350 cm^{-1} is due to the unorganized carbon, involving lattice defects while at 1600 cm^{-1} is due to the E_{2g} symmetric mode vibration in graphite. In addition, the free carbon vibration bands become shaper with the pyrolysis temperature increasing, due to the better organization state of the free carbon phase. The results further confirm the existence of free carbon in the AZ-derived ceramics, which is also observed in the XRD patterns (Fig. 7). As a result, the AZ-derived ceramics are composed of SiC/ZrC/C composites.

The effect of Cp_2ZrCl_2 content in feed on the 1600 °C ceramics was also investigated by XRD (Fig. 9). As the Cp_2ZrCl_2 content increases, the intensity of cubic ZrC peaks significantly increases, which matches very well the Zr content in ceramics determined by EDS (Fig. 6) and bulk chemical analysis (Table 2).

4. Conclusions

Synthesis of SiC/ZrC/C composites derived from AHPCS/Cp_2ZrCl_2 hybrid precursors was demonstrated, which involves that the hybrid precursor was prepared by blending AHPCS and Cp_2ZrCl_2, and then cross-linked at 170 °C, followed by pyrolysis at high temperatures. The cross-linking and polymer-to-ceramic conversion of as-synthesized AHPCS/Cp_2ZrCl_2 were characterized by means of FTIR, ^{13}C NMR, TGA, EDS, Raman spectroscopy and XRD. It is suggested that dehydrocoupling, hydrosilylation and dehydrochlorication are involved in the cross-linking of the hybrid precursor, which is responsible for a relatively high ceramic yield of 75.5% at 1200 °C. The polymer-to-ceramic conversion is complete at 900 °C, and it gives an amorphous ceramic. Further heating at 1350 °C induces partial crystallization, and then the characteristic peaks of β-SiC and cubic ZrC appear at 1600 °C. Herein, the present work opens a new synthetic route toward the preparation of SiC/ZrC/C ceramics based on the use of AHPCS/Cp_2ZrCl_2 hybrid precursor. The microstructure and properties of the as-synthesized SiC/ZrC/C ceramics will be published in the near future.

Acknowledgments

The project was supported by National Natural Science Foundation of China (Nos. 50802079 and 51072169), and Natural Science Foundation of Fujian Province of China (No. 2011J01330).

References

1. Sneddon LG, Pender MJ, Forsthoefel KM, Kusari U, Wei XL. Design, syntheses and applications of chemical precursors to advanced ceramic materials in nanostructured forms. *J Eur Ceram Soc* 2005;**25**:91–7.
2. Yamaoka H, Ishikawa T, Kumagawa K. Excellent heat resistance of Si—Zr—C—O fibre. *J Mater Sci* 1999;**34**:1333–9.
3. Chernikov A, Kosukhin V. Deposition of ZrC coats on UO_2 particles using the chloride process. *Nucl Eng Des* 2008;**238**:2861–5.
4. Opeka MM, Talmy IG, Wuchina EJ, Zaykoski JA, Causey SJ. Mechanical, thermal and oxidation properties of refractory hafnium and zirconium compounds. *J Eur Ceram Soc* 1999;**19**:2405–14.
5. Pizona D, Lucas R, Chehaidia S, Foucauda S, Maîtrea A. From trimethylvinyl-silane to ZrC–SiC hybrid materials. *J Eur Ceram Soc* 2011;**31**:2687–90.
6. Corriu R, Gerbier P, Guerin C, Henner B. The thermal conversion of poly[(silylene)-diacetylene] metal oxide composites: a new approach to β-SiC–MC ceramics. *Angew Chem Int Ed Engl* 1992;**31**: 1195–7.
7. Corriu RJP. Ceramics and nanostructures from molecular precursors. *Angew Chem Int Ed Engl* 2000;**39**:1376–98.
8. Corriu RJP, Gerbier P, Guerin C, Henner B. Poly[(silylene)diacetylene]/finemetal oxide powder dispersions: use as precursors to silicon-based compositeceramics. *J Mater Chem* 2000;**10**:2173–82.
9. Ishikawa T, Kohtoku Y, Kumagawa K. Production mechanism of polyzirconocarbosilane using zirconium(IV)acetylacetonate and its conversion of the polymer into inorganic materials. *J Mater Sci* 1998;**33**:161–6.
10. Tsirlin AM, Shcherbakova GI, Florina EK, Popova NA, Gubin SP, Moroz EM, et al. Nano-structured metal-containing polymer precursors for high temperature non-oxide ceramics and ceramic fibers-syntheses, pyrolyses and properties. *J Eur Ceram Soc* 2002;**22**:2577–85.
11. Amoros P, Beltran D, Guillem C, Latorre J. Synthesis and characterization of SiC/MC/C Ceramics (M = Ti, Zr, Hf) starting from totally non-oxidic precursors. *Chem Mater* 2002;**14**:1585–90.
12. Interrante LV, Shen QH. In: Dvornic PR, Owen MJ, editors. *Silicon-containing dendritic polymers*. Dordrecht: Springer; 2009 [chapter 12].
13. Huang TH, Yu ZJ, He XM, Huang MH, Chen LF, Xia HP, et al. One-pot synthesis and characterization of a new, branched polycarbosilane bearing allyl groups. *Chin Chem Lett* 2007;**18**:754–7.
14. Huang MH, Fang YH, Li R, Huang TH, Yu ZJ, Xia HP. Synthesis and properties of liquid polycarbosilanes with hyperbranched structures. *J Appl Polym Sci* 2009;**113**:1611–8.
15. Fang YH, Huang MH, Yu ZJ, Xia HP, Chen LF, Zhang Y, et al. Synthesis, characterization, and pyrolytic conversion of a novel liquid polycarbosilane. *J Am Ceram Soc* 2008;**91**:3298–302.
16. Yu ZJ, Li R, Zhan JY, Zhou C, Yang L, He GM, et al. Synthesis and characterization of a propargyl-substituted polycarbosilane with high ceramic yield. *J Appl Polym Sci* 2011;**121**:3400–6.
17. Li HB, Zhang LT, Cheng LF, Wang YG, Yu ZJ, Huang MH, et al. Polymer–ceramic conversion of a highly branched liquid polycarbosilane for SiC-based ceramics. *J Mater Sci* 2008;**43**:2806–11.
18. Li HB, Zhang LT, Cheng LF, Wang YG, Yu ZJ, Huang MH, et al. Effect of the polycarbosilane structure on its final ceramic yield. *J Eur Ceram Soc* 2008;**28**:887–91.
19. Li HB, Zhang LT, Cheng LF, Yu ZJ, Huang MH, Tu HB, et al. Effect of curing and pyrolysis processing on the ceramic yield of a highly branched polycarbosilane. *J Mater Sci* 2009;**44**:721–5.
20. Cho MS, Kim BH, Kong JI, Sung AY, Woo HG. Synthesis, catalytic Si···Si dehydrocoupling, and thermolysis of polyvinylsilanes $[CH_2CH(SiH_2X)]_n$ (X = H, Ph). *J Organomet Chem* 2003;**685**:99–106.
21. Corey JY, Rooney SM. Reactions of symmetrical and unsymmetrical disilanes in the presence of $Cp_2MCl_2/^nBuLi$ (M = Ti, Zr, Hf). *J Organomet Chem* 1996;**521**:75–91.
22. Horacek M, Pinkas J, Gyepes R, Kubista J, Mach K. Reactivity of $SiMe_2H$ substituents in permethylated titanocene complexes: dehydrocoupling and ethene hydrosilylation. *Organometallics* 2008;**27**: 2635–42.
23. Takahashi T, Hasegawa M, Suzuki N, Saburi M, Rousset CJ, Fanwick PE, et al. Zirconium-catalyzed highly regioselective hydrosilation reaction of alkenes and X-ray structures of silyl(hydrido)zirconocene derivatives. *J Am Chem Soc* 1991;**113**:8564–6.
24. Shriver DF, Drezdzon MA, editors. *The manipulation of air sensitive compounds*. New York: Wiley; 1986.
25. Kumagawa K, Yamaoka H, Shibuya M, Yamamura T. Fabrication and mechanical properties of new improved Si—M—C—(O) tyranno fiber. *Ceram Eng Sci Proc* 1998;**19**:65–72.

26. Bianchini D, Barsan MM, Butler IS, Galland GB, dos Santos JHZ, Fasce DP, et al. Vibrational spectra of silsesquioxanes impregnated with the metallocene catalyst bis((η^5-cyclopentadienyl)zirconium(IV) dichloride. *Spectrochim Acta A* 2007;**68**:956–69.
27. Beck S, Brough AR, Bochmann M. α-Zirconium phosphonates as new supports for metallocene catalysts. *J Mol Catal A: Chem* 2004;**220**:275–84.
28. Puerta AR, Remsen EE, Bradley MG, Sherwood W, Sneddon LG. Synthesis and ceramic conversion reactions of 9-BBN-modified allylhydridopolycarbosilane: a new single-source precursor to boron-modified silicon carbide. *Chem Mater* 2003;**15**:478–85.
29. Wang Y, Alsmeyer DC, McCreery RL. Raman spectroscopy of carbon materials: structural basis of observed spectra. *Chem Mater* 1990;**2**: 557–63.
30. Trass S, Motz G, Rossler E, Ziegler G. Characterization of the free-carbon phase in precursor-derived Si—C—N ceramics: I, spectroscopic methods. *J Am Ceram Soc* 2002;**85**:239–44.